Whispering gallery modes in open quantum billiards

R. G Nazmitdinov,[1,2,*] K. N. Pichugin,[3,†] I. Rotter,[1,‡] and P. Šeba[3,4,§]
[1]*Max-Planck-Institut für Physik komplexer Systeme, D-01187 Dresden, Germany*
[2]*Joint Institute for Nuclear Research, 141980 Dubna, Russia*
[3]*Institute of Physics, Czech Academy of Sciences, Cukrovarnicka 10, 16253 Prague, Czech Republic*
[4]*Department of Physics, Pedagogical University, 50003 Hradec Kralove, Czech Republic*
(Received 3 April 2001; published 22 October 2001)

The poles of the *S* matrix and the wave functions of open two-dimensional quantum billiards with convex boundary of different shape are calculated by using the method of complex scaling. Two leads are attached to the cavities. The conductance of the cavities is calculated at energies with one, two, and three open channels in each lead. Bands of overlapping resonance states appear that are localized along the convex boundary of the cavities and contribute coherently to the conductance. These bands correspond to the whispering gallery modes known from classical calculations.

DOI: 10.1103/PhysRevE.64.056214 PACS number(s): 05.45.−a, 03.65.−w, 05.60.−k, 85.35.−p

The physics of nanoscale systems has advanced rapidly over the last few years. A consistent description of these small systems is a challenging task for quantum theory since their properties may be influenced strongly by attaching leads to them [1–9]. They are simulated often by means of quantum billiards. When the cavity is not fully opened, the propagation of the modes is restricted to energies at which the overlap integral between the wave functions of the resonance states and the channel wave functions is nonvanishing. In the case of well isolated resonances, the electron can propagate, therefore, only at the energies of the resonance states (''resonance tunneling''). Due to the coupling between the internal states of the cavity and the channel modes, the states get widths. When the coupling is sufficiently strong, the resonances start to overlap and to interact via channel modes. As a consequence, some redistribution in the resonance states of the cavity takes place. It reflects the transition from the spreading of K channel modes over the N resonance states of the cavity at small opening to their free propagation at large opening. In the last case, $N-K$ resonance states are (practically) decoupled from the channel while only K of them are coupled strongly leading to a maximum propagation of the K waves in the cavity. An illustration for $K=1$ is shown in Ref. [9]. This transition, called resonance trapping [10], has been studied theoretically in many different systems such as nuclei, atoms, and molecules (for references see Ref. [8]). In microwave cavities, it is traced as a function of the opening of the cavity theoretically [5,6,8] as well as experimentally [11].

The role of the structure of the cavity states themselves in the redistribution process is almost not studied up to now. We will show in the following that the interplay between the structure of the cavity states and the one-to-one alignment of a few states with channels characterizes the situation when the lead has a smaller extension than the cavity. Such a case is intermediate between the two limiting cases discussed above. The examples we consider are cavities with a convex boundary that are discussed recently in optical and other devices [12,13]. In these systems, whispering gallery modes (WGM) are known to appear classically. We show that in the quantum mechanical calculations, a certain number $N_1>K$ of resonance states overlap, couple with similar strength to the channels in both leads while $N_2=N-N_1$ ones are almost decoupled from the channels by resonance trapping. The N_1 states are localized near the convex boundary in contrast to the other ones. The localized states correspond to the WGM and cause an increased conduction (or reflection) of the quantum billiard.

The properties of open quantum systems are described usually by means of the poles of the *S* matrix. The resonance part of the *S* matrix reads [8,10]

$$S_{cc'}=i\sum_{R=1}^{N}\frac{\tilde{\gamma}_{Rc'}\tilde{\gamma}_{Rc}}{E-\tilde{E}_R+\frac{i}{2}\tilde{\Gamma}_R}, \tag{1}$$

where the $\tilde{\mathcal{E}}_R=\tilde{E}_R-(i/2)\tilde{\Gamma}_R$ are the (energy dependent) eigenenergies of the effective Hamilton operator $\mathcal{H}=\mathcal{H}_0+W$ of the open quantum billiard, $\mathcal{H}_0$ is the Hamiltonian of the closed cavity and the

$$W_{R'R}=\frac{1}{2\pi}\sum_{c=1}^{\Lambda}\mathrm{P}\int_{\epsilon_c}^{\infty}dE'\frac{\tilde{\gamma}_{Rc}\tilde{\gamma}_{R'c}}{E-E'}-\frac{i}{2}\sum_{c=1}^{\Lambda}\tilde{\gamma}_{Rc}\tilde{\gamma}_{R'c}, \tag{2}$$

are complex, generally, [14]. Equation (1) is true also for overlapping resonances [10]. The poles of the *S* matrix correspond to the solutions of the fixed-point equations $\mathcal{E}_R\equiv E_R-(i/2)\Gamma_R=\tilde{E}_R(E=E_R)-(i/2)\tilde{\Gamma}_R(E=E_R)$ and determine the energies E_R and widths Γ_R of the resonance states. The γ_{Rc} ($\tilde{\gamma}_{Rc}$) are the energy dependent coupling matrix elements between the eigenfunctions Φ_R of $\mathcal{H}_0$ (eigenfunctions $\tilde{\Phi}_R$ of $\mathcal{H}$) and the channel modes. The $\tilde{\gamma}_{Rc}$ determine, together with the values $\tilde{\mathcal{E}}_R(E)$, the transmission $\Sigma|S^{(ij)}_{c_ic_j}|^2$

*Email address: rashid@thsun1.jinr.ru
†Present address: Kirensky Institute of Physics, 660036 Krasnoyarsk, Russia. Email address: pichugin@fzu.cz
‡Email address: rotter@mpipks-dresden.mpg.de
§Email address: petr.seba@uhk.cz

from lead i to lead $j \neq i$ and the reflection $\Sigma|S^{(ii)}_{c_i c_i'}|^2$ in the lead i at the energy E. It is $\tilde{\gamma}_{Rc} \approx \gamma_{Rc}$ only for isolated resonances.

In our calculations, we find the poles of the S matrix and the wave functions $\tilde{\Phi}_R$ of the resonance states by using the method of exterior complex scaling together with the finite element method. For details see Refs. [5,6]. The conductance is calculated from the Schrödinger equation for the closed cavity that is modified by the boundary conditions due to attaching the leads, see Ref. [15].

We performed calculations for three small flat resonators of different shape with comparable area: a semicircle as an example for an almost regular cavity, a semicircle with an internal scatterer (SIS), and a semi-Bunimovich billiard as examples for more chaotic cavities. Every resonator is coupled to two leads, see Figs. 1(c)–1(j) for the SIS. The eigenvalue pictures are very similar to one another in all three cases. There are different groups of poles [see Fig. 1(a)]: one group is very near to the real axis while the other ones are lying deep in the complex plane. The states near to the real axis are trapped by those of the other groups.

The short-lived states start at the opening of thresholds lying at $E=\pi^2$, $(2\pi)^2$ and $(3\pi)^2$. They form bands of overlapping resonance states, i.e., their widths are larger than their distance in energy. The states of the band A appear when the first channel opens. They are coupled strongly to the open channel in each of both leads [Figs. 1(c), 1(d), and 1(g)]. At $E=(2\pi)^2$, the second band (B) of poles starts whose wave functions are related to two channels in each lead [Figs. 1(e) and 1(h)]. Here, also another group $B1$ of states arises the widths of which increase first but then decrease with increasing energy [Fig. 1(f)]. The bands A and B continue to higher energy while a new band (C) starts at $E=(3\pi)^2$ where the third threshold opens. The wave functions of these states are related to three channels in every lead [Fig. 1(i)]. Also here, another group ($C1$) of states appears whose widths first increase but then decrease with increasing energy [Fig. 1(j)].

In all three cases studied by us (semi-Bunimovich and semicircle billiards), the structure of the cavity states plays an important role in the trapping process. The most interesting result is the localization of the wave functions of the states belonging to the bands A, B, and C, called WGM in the following. The first WGM is pushed in direction to the border of the cavity at higher energies while the second one is parallel to it. Even some hint to a third WGM can be seen when three channels are open at $E>(3\pi)^2$. In contrast to the WGM, the long-lived states are spread over the whole cavity.

The WGM are characteristic of the closed systems considered by us. Attaching the leads to the cavities as shown in Fig. 1, the WGM get large coupling matrix elements γ_{Rc} in relation to the channels c. When the cavities become opened, the widths $\tilde{\Gamma}_R$ of the WGM can further increase by trapping the other resonance states. The states belonging to the WGM form bands with a (nearly) square root dependence on energy.

In Fig. 2(a), we show the eigenvalue picture for the SIS whose convex surface is distorted by a cut [Fig. 2(g)]. There are two groups of short-lived states corresponding to the fact that the WGM splits, by the distorting cut, into two parts with different lengths of the ''ways'' for reflection in channel 1 and 2. The two separated parts of the WGM can be seen in the wave functions of these states. One example is shown in Fig. 2(g).

The eigenvalue picture shown in Fig. 2(c) corresponds to the SIS with a shifted position $s=1$ of one of the leads, see Fig. 2(h). Also this eigenvalue picture shows some band structure. The states of the band A split into two parts: the localized part (related to the WGM) is coupled more strongly to the unshifted lead than to the shifted one while the other (not localized) part, arising from the ''sea'' of almost bound states, is coupled also to the shifted lead. Both parts interact strongly at higher energy where two channels are open.

The trajectories of the eigenvalues as a function of the shift s of the left lead [Fig. 2(e)] show the mechanism of resonance trapping. The widths of the WGM decrease as a function of increasing s while the widths of some states of the ''sea'' of almost bound states increase according to the sum rule $\Sigma\tilde{\Gamma}_R(E)=\text{const}$. In the neighborhood of $s=2.5$, resonance trapping occurs between the latter states: the widths of three states become maximum at $s=2.5$ by trapping the other ones that again approach the real axis at this value of s. The wave functions of the short-lived states have a clear bouncing-ball structure [Fig. 2(i)]. The poles of the WGM are almost independent of s in the neighborhood of $s=2.5$ and their wave functions have kept their WGM structure [Fig. 2(j)]. The bouncing-ball structure is less stable than the WGM one since the degree of overlapping of the poles is smaller [Fig. 2(e)].

The properties of the resonance states are reflected, at least partly, in the conductivity of the cavity. According to Eq. (1), the maximum value of the matrix element $S^{(ij)}_{cc}$ is reached for $\tilde{\gamma}^{(i)}_{Rc} \approx \tilde{\gamma}^{(j)}_{Rc}$ $(j \neq i)$. While single short-lived states formed by resonance trapping are aligned each with one channel and $\tilde{\gamma}_{Rc'} \ll \tilde{\gamma}_{Rc}$, each of the two states R and R' is coupled to both channels with almost the same strength when the poles overlap ($\mathcal{E}_{R'} \approx \mathcal{E}_R$) as the poles of the WGM do. The WGM are expected, therefore, to cause a large conductance of the cavity when the leads are attached symmetrically.

In Fig. 1(b), the conductivity of the SIS is shown as a function of energy. The coherent structure of the conductance in the energy interval between the two lowest thresholds can be seen clearly. The mean value of the conductance is about 0.9 in the energy interval between the two lowest thresholds. In the next higher energy region, the value of the conductance is never smaller than 1 meaning that the wave is reflected into one channel, at the most.

We calculated also the conductance and reflection of the SIS, when its shape is distorted either by a cut in the circular boundary of the cavity [Fig. 2(b)] or by a somewhat shifted position of one of the leads [Fig. 2(d)]. The reflection shows, in the first case, the same coherent structure as the conductance in the undistorted case. The mean value is large in the energy regions considered. In the other case, the conductance decreases strongly with energy in the interval between the

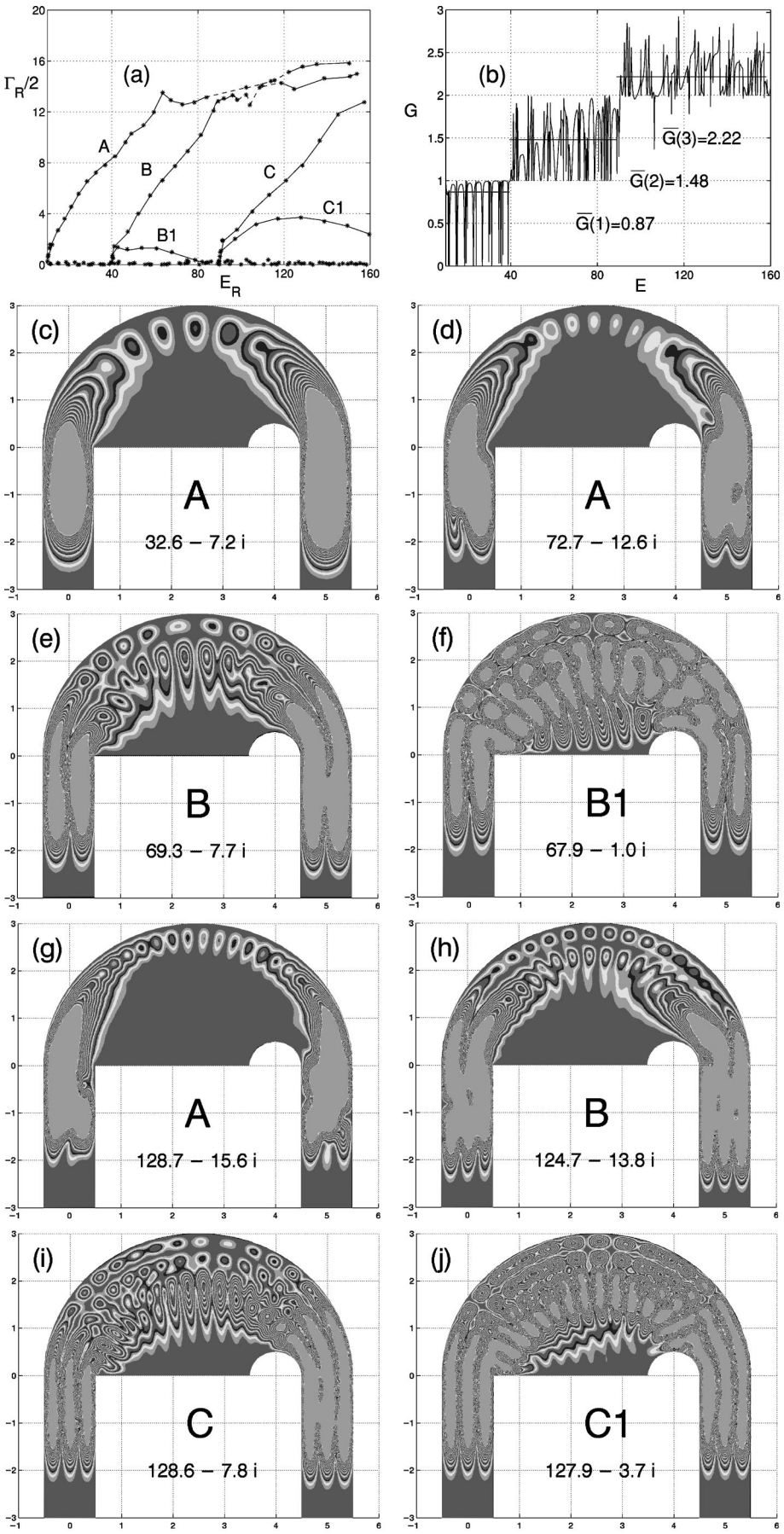

FIG. 1. The poles of the S matrix (a) and conductance $G=\Sigma|S^{(ij)}_{c_i c_j}|^2$ (b) for the SIS. The poles of the S matrix (denoted by stars) are connected by lines for guiding the eyes. The full lines in (b) show the mean value of the conductivity between every two thresholds. Some wave functions ($|\tilde{\Phi}_R|^2$) of the SIS: (c) from band A of the first energy interval $\pi^2<E<(2\pi)^2$, (d), (e), and (f) from bands A, B, and $B1$ of the second energy interval $(2\pi)^2<E<(3\pi)^2$, (g), (h), (i), and (j) from bands A, B, C, and $C1$ of the third energy interval $(3\pi)^2<E<(4\pi)^2$. The energies E_R and widths Γ_R are in units $\hbar^2/(2md^2)$ where $d=1$ is the width of the attached waveguide.

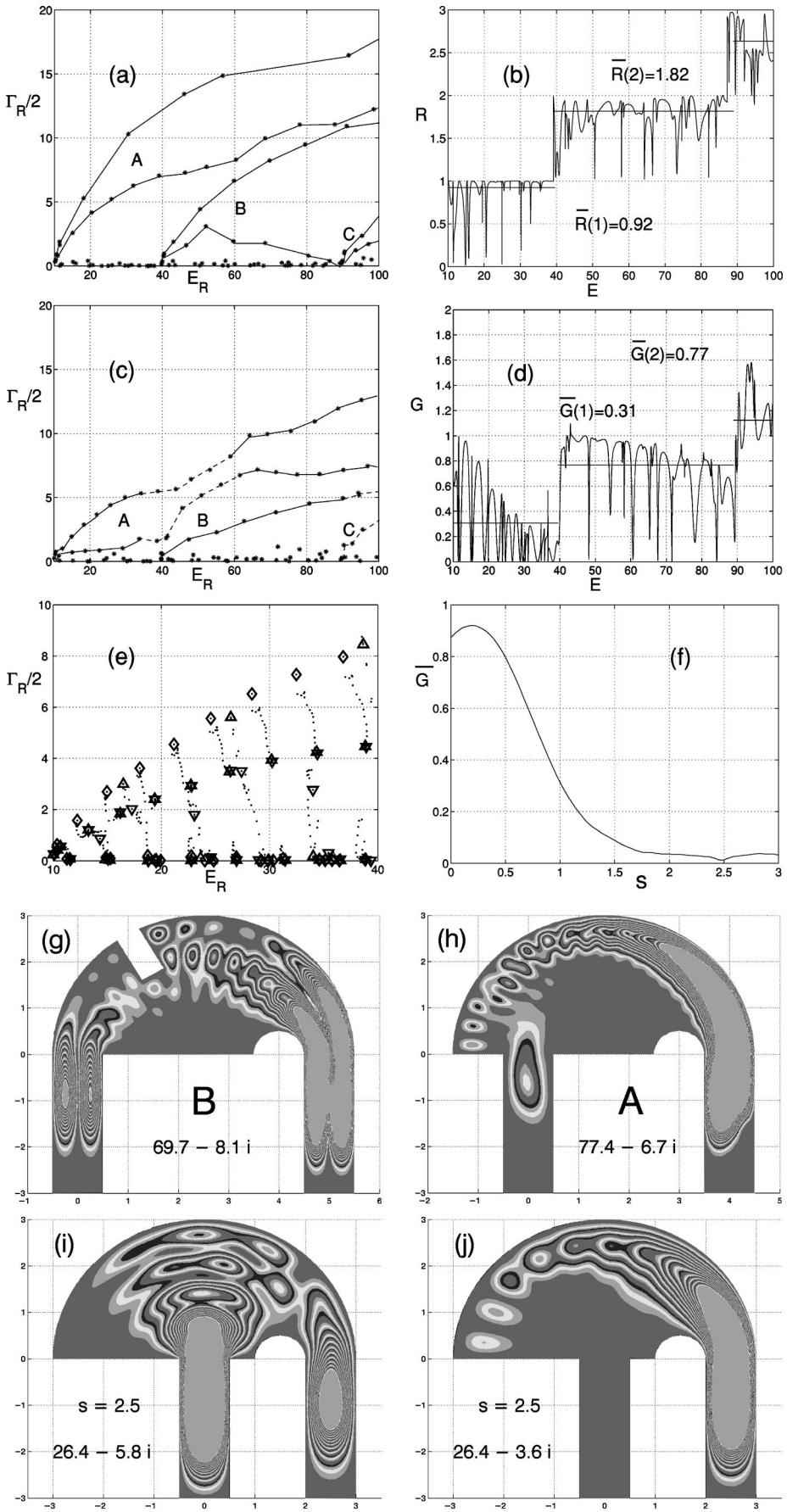

FIG. 2. The poles of the S matrix (a),(c), reflection $R=\Sigma|S^{(ii)}_{c_i c'_i}|^2$, (b) and conductance $G=\Sigma|S^{(ij)}_{c_i c_j}|^2$ (d) for the SIS distorted by a cut in the circular boundary of the cavity (a),(b) and by a somewhat shifted position of one of the leads (c),(d). One wave function ($|\tilde{\Phi}_R|^2$) for each case is shown in (g) and (h). The trajectories of the poles of the S matrix (e) and the mean value $\overline{G}$ of the conductance (f) as a function of the position s of the left lead. In (e), the poles at the positions $s=0$, 2.5, 3 are marked with $\diamond$, $\triangle$ and $\triangledown$. Two wave functions (i),(j) at $s=2.5$. For further explanations see Fig. 1.

first and second threshold. This is caused by the fact that modes with higher energy are localized nearer to the convex boundary of the cavity than those with lower energy. This result is supported by the behavior of the conductance at higher energy that does not exceed the maximum value of the conductance of a one-channel case. The conductance as a function of the position of one of the leads [Fig. 2(f)] decreases strongly with approaching the bouncing-ball situation ($s=2.5$). Here, reflection is maximum.

To shed light on the quantum mechanical results we consider the classical motion of a free particle inside billiards with the same geometry as discussed above. The potential is assumed to be zero inside the billiard and the boundaries are mirrors for the motion of the particle along trajectories calculated from the laws of geometrical optics. The dynamics of the motion can be reduced to a canonical mapping in Birkhoff coordinates (q,p), [16] which is a Poincaré mapping at the boundary of the billiard. The coordinate q is that of the arc length at the boundary of the billiard where the bounce takes place, and $p_t=\mathbf{p}\cdot\mathbf{t}/|\mathbf{p}|$ is the tangential momentum at this point. Each trajectory starts at some arbitrary initial point (x_0,y_0) of the attached leads with an angle α_0 characterizing the direction of the motion. The trajectories that run close to the convex boundary of our billiard and accumulate upon it are defined as the WGM of the billiard. These trajectories occupy the major part of the surface of section as can be seen from Fig. 3 for the SIS. The symmetry of the chosen geometry is reflected in the mapping of the regions corresponding to a different number of bounces at the boundary. Additionally, we calculated the ratio of the number of trajectories of the WGM to the total number of trajectories passing through the billiard. This ratio is about 60% for the semicircle and about 70% for the SIS, since the non-WGM trajectories are hindered by the scatterer inside the cavity. This result supports the idea that the WGM give the main contribution to the conductance. Further, a billiard with a convex boundary possesses a family of invariant tori that correspond to the motion close to the boundary [17]. In our quantum mechanical simulations, the wave functions of the states of the WGM band are localized close to the convex boundary in the closed systems and remain localized when the systems are opened to a few channels by attaching leads to them. Thus, the classical results are in qualitative agreement with the quantum-mechanical ones.

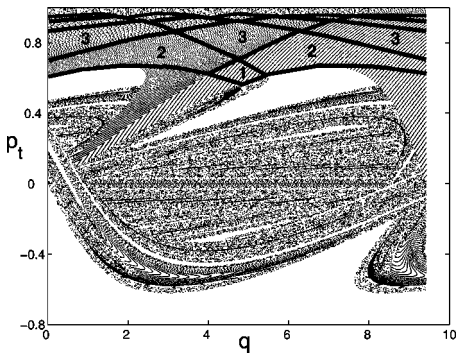

FIG. 3. Classical Poincaré section for the SIS in the Birkhoff variables: tangential momentum p_t vs arc length q. The trajectories of the WGM are distinguished according to the number m of bounces at the boundary for $m\leqslant 5$.

Summarizing the results, we state the following. In open quantum cavities with convex boundary, the structure of the wave functions of the cavity states plays an important role in the trapping process. Some resonance states receive large widths by trapping the remaining ones, form bands of overlapping resonance states, and are localized near the convex boundary of the cavity. These bands correspond to the WGM known from classical calculations for different systems with convex boundary. When two leads are attached symmetrically to the cavity, the WGM are coupled to both leads with almost the same strength. WGM-like structures exist in relation to every open channel in the two waveguides. The WGM are responsible for a high conductivity that decreases dramatically when the symmetry of the system is distorted. This fact can be used surely for the design of quantum cavities in practical applications.

[1] C. Beenakker, Rev. Mod. Phys. **69**, 731 (1997).
[2] Y. Alhassid, Rev. Mod. Phys. **72**, 895 (2000).
[3] L. Wirtz, J-Z. Tang, and J. Burgdörfer, Phys. Rev. B **59**, 2956 (1999); S. Rotter, J-Z. Tang, L. Wirtz, J. Trost, and J. Burgdörfer, *ibid.* **62**, 1950 (2000).
[4] I. V. Zozoulenko, R. Schuster, K. F. Berggren, and K. Ensslin, Phys. Rev. B **55**, R10 209 (1997); T. Blomquist and I. V. Zozoulenko, *ibid.* **61**, 1724 (2000).
[5] E. Persson, K. Pichugin, I. Rotter, and P. Šeba, Phys. Rev. E **58**, 8001 (1998).
[6] P. Šeba, I. Rotter, M. Müller, E. Persson, and K. Pichugin, Phys. Rev. E **61**, 66 (2000).
[7] S. Ree and L. E. Reichi, Phys. Rev. B **59**, 8163 (1999).
[8] I. Rotter, E. Persson, K. Pichugin, and P. Šeba, Phys. Rev. E **62**, 450 (2000).
[9] G. Akguc and L. Reichl, Phys. Rev. E **64**, 036213 (2001).
[10] I. Rotter, Rep. Prog. Phys. **54**, 635 (1991); e-print quant-ph/0105068 [Phys. Rev. E, (to be published)].
[11] E. Persson, I. Rotter, H. J. Stöckmann, and M. Barth, Phys. Rev. Lett. **85**, 2478 (2000).
[12] J. U. Nöckel and A. D. Stone, Nature (London) **385**, 45 (1997).
[13] R. E. Prange, R. Narevich, and O. Zaitsev, e-print nlin.CD/0010001.
[14] S. Drożdż, J. Okolowicz, M. Ploszajczak, and I. Rotter, Phys. Rev. C **62**, 024313 (2000).
[15] T. Ando, Phys. Rev. B **44**, 8017 (1991).
[16] V. I Arnold and A. Avez, *Ergodic Problems of Classical Mechanics* (Addison-Wesley, Reading, MA, 1989).
[17] V. F. Lazutkin, *KAM Theory and Semiclassical Approximations to Eigenfunctions* (Springer, Berlin, 1991).